

# Magnetic flux supplement to coronal bright points

CHAOZHOU MOU<sup>1</sup>, ZHENGHUA HUANG<sup>1</sup>, LIDONG XIA<sup>1</sup>, MARIA S. MADJARSKA<sup>2</sup>, BO LI<sup>1</sup>, HUI FU<sup>1</sup>,  
FANGRAN JIAO<sup>1</sup>, ZHENYONG HOU<sup>1</sup>

Received date, accepted date

## ABSTRACT

Coronal bright points (BPs) are associated with magnetic bipolar features (MBFs) and magnetic cancellation. Here, we investigate how BP-associated MBFs form and how the consequent magnetic cancellation occurs. We analyse longitudinal magnetograms from the Helioseismic and Magnetic Imager to investigate the photospheric magnetic flux evolution of 70 BPs. From images taken in the 193 Å passband of the Atmospheric Imaging Assembly (AIA) we determine that the BPs' lifetimes vary from 2.7 to 58.8 hours. The formation of the BP MBFs is found to involve three processes, namely emergence, convergence and local coalescence of the magnetic fluxes. The formation of a MBF can involve more than one of these processes. Out of the 70 cases, flux emergence is the main process of a MBF buildup of 52 BPs, mainly convergence is seen in 28, and 14 cases are associated with local coalescence. For MBFs formed by bipolar emergence, the time difference between the flux emergence and the BP appearance in the AIA 193 Å passband varies from 0.1 to 3.2 hours with an average of 1.3 hours. While magnetic cancellation is found in all 70 BPs, it can occur in three different ways: (I) between a MBF and small weak magnetic features (in 33 BPs); (II) within a MBF with the two polarities moving towards each other from a large distance (34 BPs); (III) within a MBF whose two main polarities emerge in the same place simultaneously (3 BPs). While a MBF builds up the skeleton of a BP, we find that the magnetic activities responsible for the BP heating may involve small weak fields.

*Subject headings:* Sun: activity - Sun: corona - Sun: magnetic fields - Method: observational

## 1. Introduction

Coronal bright points (BPs) are small (on average 20''–30'') and short-lived (from a few minutes to a few tens of hours) bright structures, ubiquitously found in the solar corona. They are believed to be the signature of a direct energy deposition in the upper solar atmosphere (Webb et al. 1993; McIntosh 2007). Coronal BPs were first identified in X-ray images and were named X-ray bright points (XBPs) in the 1970s (Vaiana et al. 1970). They have an average lifetime of 8 hours in X-rays (Timothy et al. 1974; Golub et al. 1976a,b). When observed in Extreme Ultra-violet (EUV) (e.g. Habbal & Withbroe 1981; Habbal et al. 1988; Zhang et al. 2001; Madjarska et al.

2012, etc.), they are found to have a lifetime that varies from a few minutes to a few days with an average of 20 hours (Zhang et al. 2001). BPs consist of multiple small-scale (a few arcseconds) and rapidly-evolving (a few minutes) loops (e.g. Sheeley & Golub 1979; Habbal et al. 1990; Ugarte-Urra & Doyle 2004).

Many studies (e.g. Krieger et al. 1971; Golub et al. 1975a,b, 1976a, 1977; Webb et al. 1993; Brown et al. 2001; Madjarska et al. 2003; Huang et al. 2012; Chandrashekhar et al. 2013, etc.) have revealed that BPs are associated with magnetic bipolar features (MBFs). A MBF is a pair of opposite-polarity magnetic features observed in magnetogram data. The relationship between magnetic flux emergence and BPs has been studied in the past but only limited case studies were reported during the Solar Heliospheric Observatory (SoHO) era. Golub et al. (1977) compared BPs observed in X-rays with ephemeral active regions (i.e. emerging bipolar regions) and found a weak correlation.

<sup>1</sup>Shandong Provincial Key Laboratory of Optical Astronomy and Solar-Terrestrial Environment, Institute of Space Sciences, Shandong University, Weihai, 264209 Shandong, China  
z.huang@sdu.edu.cn

<sup>2</sup>Armagh Observatory, College Hill, Armagh BT61 9DG, UK

Martin & Harvey (1979) argued that the discrepancy can be explained if the BPs are associated with short-lived ephemeral active regions that might not have been detected in the low temporal resolution data. BPs are also strongly associated with magnetic cancellation (e.g. Webb et al. 1993; Brown et al. 2001; Madjarska et al. 2003; Huang et al. 2012, etc.). A study by Webb et al. (1993) found that 18 of 25 BPs were associated with magnetic cancellation. They also found that BPs have a stronger connection with magnetic cancellation rather than flux emergence. From high resolution Solar Optical Telescope (SOT) magnetograms, Huang et al. (2012) determined that all 28 BPs were associated with flux emergence followed by magnetic field cancellation.

The strong connection between BPs and magnetic field cancellation has been considered as evidence of magnetic reconnection occurring in BPs. Preš & Phillips (1999) suggested that all the energy losses of a BP are in fact replenished by magnetic energy. Magnetic reconnection in BPs has also been supported by a magnetic field dynamic reconfiguration of BP (Pérez-Suárez et al. 2008; Alexander et al. 2011; Zhang et al. 2012). Recently, Zhang et al. (2014) suggested that interchange reconnection might occur between two close chambers of a BP. Priest et al. (1994) proposed a scenario where the reconnection results from the converging motion of magnetic polarities. According to this model, the interaction distance has to be less than a certain value in order to trigger the appearance of a BP. This model was also further developed by Parnell et al. (1994) and von Rekowski et al. (2006a,b), and it was linked to various observations (e.g. Brown et al. 2001; Madjarska et al. 2003; Zhang et al. 2012; Huang et al. 2012, etc.).

Although BPs have been studied since the 1970s, many open questions remain. Firstly, how does a BP-associated MBF form? This question has not been answered because high-resolution and high-cadence magnetic field observations in the past were taken for a limit period of time (hours) and had a limited FOV. For instance, the high-resolution observations by the Magnetic Doppler Imager onboard SoHO were restricted only to the disk center region, had a limited field-of-view (FOV) and were only occasionally coordinated with the highest spatial resolution (in the past) coronal imager, the Transition Region And Coronal Explorer (TRACE). In contrast, the Helioseismic and Magnetic Imager (HMI) onboard the Solar Dynamics Observatory (SDO) provides constantly-taken full-disk longi-

tudinal magnetograms at 45 s cadence together with a 12 s cadence imaging of the solar atmosphere by the Atmospheric Imaging Assembly (AIA). Secondly, it is not yet known whether magnetic cancellation associated with BPs occurs only between the two main polarities of the BP MBF or whether small-scale magnetic fluxes that emerge/evolve in the vicinity of the MBF are also involved? These questions are crucial for the understanding on how BPs are formed and heated to coronal temperatures. In the present study, we use the AIA data to identify BPs and analyse HMI magnetograms to investigate their magnetic field evolution. The article is organised as follows: In Section 2, we describe the observations and the data analysis. The results are presented in Section 3. The discussion and conclusions are given in Section 4.

## 2. Observations and analysis

The data used in the present study were taken by the AIA (Lemen et al. 2012) and the HMI (Scherrer et al. 2012) onboard SDO (Pesnell et al. 2012). The AIA data have a 12 s cadence and 1.2'' spatial resolution. The HMI longitudinal magnetograms used in this study are obtained at 45 s cadence and have  $\sim 1''$  spatial resolution. The noise level of the HMI data is  $\sim 10 \text{ Mx cm}^{-2}$  (Liu et al. 2012). The data used in this study were taken from 2010 December 31, 12:00 UT to 2011 January 04, 00:00 UT, i.e. 84 hours in total.

The AIA and HMI data were reduced using the IDL routine *aia\_prep.pro*. The AIA 1600 Å and 304 Å images were used to examine the alignment between the AIA 193 Å images and the HMI magnetograms. We found that *aia\_prep.pro* has performed an alignment of the two instruments with an accuracy better than 3''. We first identified each BP in the AIA 193 Å images, then searched for its associated magnetic features within 20'' around the BP. We followed the evolution of each BP in the imaging data and the magnetograms to determine which magnetic features are the ones that are responsible for the BP formation and evolution.

We aim to study the magnetic field evolution of the BPs from their birth until their full disappearance. We visually identified 70 BPs. These BPs are well representative as their total emission and their associated magnetic flux distribute over a large range of values (see Section 3.1 for detail). To follow the evolution of the magnetic features, we first used automatic techniques, e.g. the Southwest Automatic Magnetic Interpretation Suite (SWAMIS, DeForest et al. 2007;

Lamb et al. 2008, 2010, 2013). SWAMIS is powerful in tracking features that satisfy a set of conditions, e.g. minimum and maximum of flux density, size and lifetime, etc. However, many cases in the present study involve small-scale magnetic elements that have various sizes and flux densities that can not be recognized by a set of input parameters in the automatic algorithms. Thus, the visual analysis was best suited for the present work.

### 3. Results and discussion

In all 70 cases, a BP detected in the AIA 193 Å images is associated with a MBF. Usually, MBFs appear as two clusters of opposite-polarity magnetic features in the HMI magnetograms and are found in the vicinity of the BPs. Please note that identification of a MBF in our study is based on the presence of a BP, i.e. a BP is firstly identified and the corresponding MBF is identified after. For each case we traced back the evolution of the MBF and the surrounding flux concentrations 12 hours prior to the birth of the BP in order to study how a MBF is formed, and how it evolves and interacts with the surrounding magnetic features.

#### 3.1. General characteristics of BPs and their associated MBFs

Once a BP was visually identified, its AIA 193 Å lightcurve was produced. A BP lightcurve is normally spiky but the long-term evolution clearly presents a fast rising phase and a fast decaying phase (Zhang et al. 2001). Based on this, the birth and death of a BP were determined from the start of the rising phase (i.e. a sharp intensity increase with respect to the background emission) and the end of the decaying phase (i.e. a drop of the emission to the background level), respectively. The lifetimes of the 70 BPs are listed in Table 1, and a histogram is shown in Fig. 1. In AIA 193 Å, the BP lifetime ranges from 2.7 to 58.8 hours, with an average of 20.9 hours. This is consistent with the results of Zhang et al. (2001), who found a 20 hour average lifetime based on a statistical analysis of 48 EUV BPs observed in the EIT 195 Å passband that has a similar temperature response to the AIA 193 Å channel.

Similarly to Pevtsov et al. (2003), we investigate the relationship between the emission of the BPs and their total unsigned magnetic flux. In Fig. 2, we display a plot of the total AIA 193 Å radiances of the 70 BPs vs. the total unsigned magnetic fluxes of their as-

sociated MBFs. The measurements were taken at the peak of the BP radiation. The linear fit given in Fig. 2 indicates a power-law approximation of  $L_x \propto \Phi^{1.37}$ , where  $L_x$  is the radiance of a BP and  $\Phi$  is its total unsigned magnetic flux of the associated MBF.

As discussed in Section 1, the distance between the two main polarities of a MBF can be used to test BP models, e.g. the convergence model by (Priest et al. 1994). To obtain objective measurements of the distance between the two polarities of the MBFs, we determined the separation between the closest points of the 30 Mx cm<sup>-2</sup> contours of the two opposite polarity magnetic features. If the two contours were in contact, the distance was defined as zero. In Fig. 3, we show the statistical results for all 70 BPs at their first appearance (left panel) and at their radiation peak (right panel) in AIA 193 Å. Considering the time when the BPs first appear, the distance is in the range from 0 to 31.5". A zero distance is found in 16 BP-associated MBFs, 15 of which are related to bipolar flux emergence. While the BPs are at their radiation peak, the distance spreads from 0" to 26.8" with a distribution peak at ~ 5". The distance of the two main polarities of the BPs will be further discussed in the following sections regarding the formation and evolution of MBFs.

#### 3.2. On the formation of MBFs associated with BPs

In the present work, a MBF was visually traced back 12 hours prior to the first appearance of a BP in AIA 193 Å. We found that the BP-associated MBFs can be formed via three ways: emergence, convergence and local coalescence. Magnetic flux emergence is a phenomenon which represents the appearance of a magnetic feature in magnetogram data. Convergence is a process where two pre-existing opposite magnetic polarities that are initially found at far away distances move towards each other, and a BP would appear in the AIA 193 Å images once the polarities move closer than a certain distance. It is possible that the two opposite polarities of a MBF are already connected while the distance between the polarities is still quite large. In this study we found that such a MBF can not produce a BP in the AIA 193 Å if convergence is not at work. To clarify this issue, we believe that one would need a reliable field extrapolation that is worthy to be tackled in future studies. Local magnetic coalescence is a phenomenon where a magnetic feature is formed by the merging of small-scale magnetic features (with a size close to the instrumental resolution limit) of the

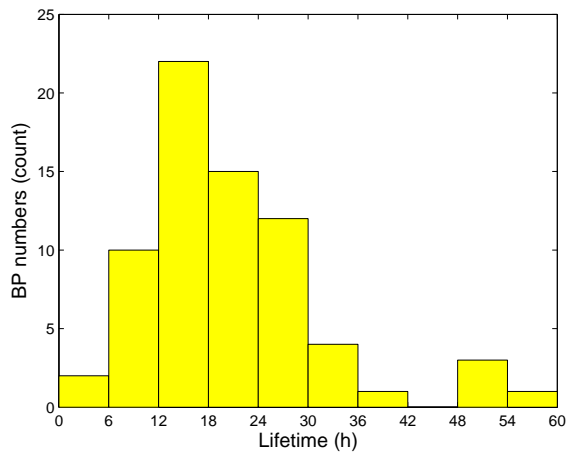


Fig. 1.— Statistical histogram of the lifetime of 70 EUV BPs. The bin size is 6 hours.

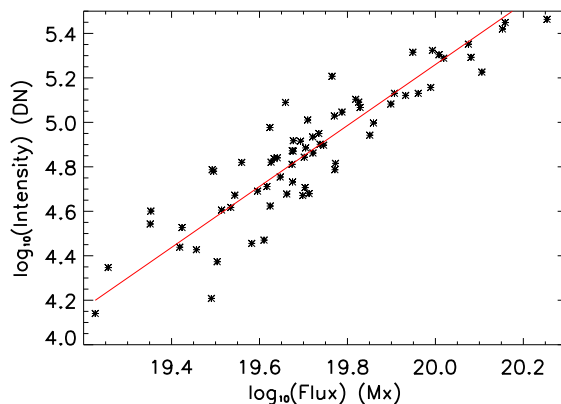


Fig. 2.— Distribution of the total AIA 193 Å radiance of the 70 BPs vs. their total unsigned magnetic flux. Both the AIA 193 Å radiance and the magnetic flux are measured at the time when the BPs reach their radiation peak. The red solid line is the linear fit of the data points.

same sign. However, our analysis shows that the two polarities of a MBF are not usually formed in a single way. For example, in some cases, a polarity formed by emergence or local coalescence moves towards a pre-existing one to form a MBF that is associated with a BP.

In Table 1, we list the formation methods for the MBFs of all 70 BPs. A Venn diagram of the statistical results is given in Fig. 4. We found that in 46 cases the two polarities are formed in the same way, in which 35 are emergence, 5 are convergence and 6 are local coalescence. The MBF formation for the remaining 24

cases involved more than one process. In summary, out of 70 BPs, emergence is found in 52 cases, convergence in 28 cases and local coalescence in 14 cases. In the following sections we give examples of these three formation processes.

### 3.2.1. A MBF formed by bipolar emergence

Fig. 5 presents the formation process of a MBF associated with the BP listed as No. 1 in Table 1. The BP is first detected at 00:04 UT on January 1 and disappears at 13:19 UT on January 2, with a total duration of 37.3 hours. The BP MBF is formed through



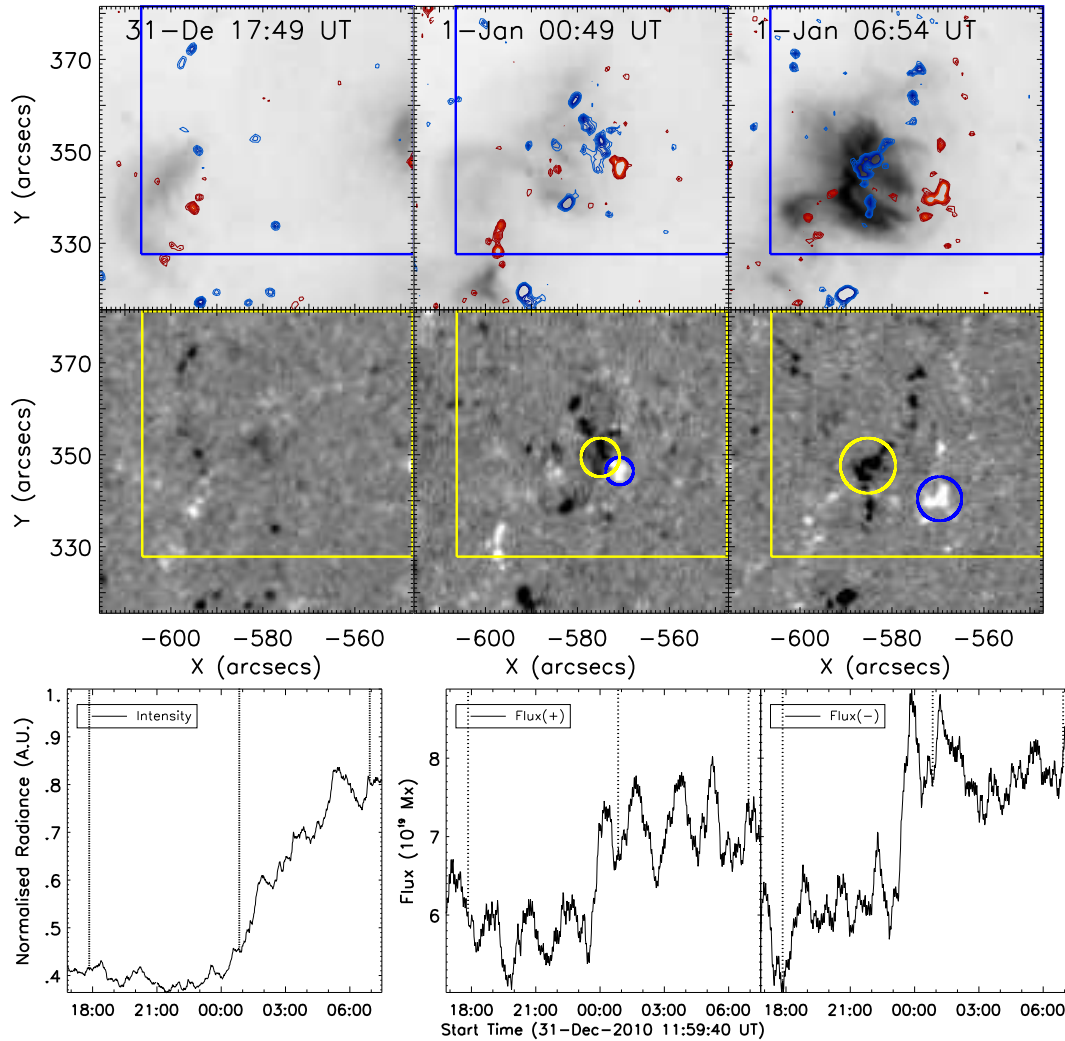


Fig. 5.— The formation process of a MBF and the associated BP (No. 1 in Table 1), which is formed by bipolar emergence. The top row gives the BP region as seen in AIA 193 Å at the indicated time. The middle row shows the corresponding HMI magnetograms. The bottom row shows the normalised AIA 193 Å lightcurve (left), and the positive (middle) and negative (right) magnetic fluxes obtained in the blue and yellow boxes marked in the top two rows. The contours of positive (red) and negative (blue) magnetic flux density are over-plotted in the top row. The yellow and blue circles over-plotted on the magnetograms denote the locations of the negative and positive polarities of the MBF. The dotted lines over-plotted in the bottom row denote the time of the images shown on the top and middle rows. An animation is enclosed online.

pears in AIA 193 Å (see the top row of Fig. 5). An animation attached to Fig. 5 clearly demonstrates this process. The AIA 193 Å lightcurve of the BP shows that a sharp intensity increase starts at approximately 00:00 UT and reaches its peak at 06:54 UT on January 1 (see left panel of the bottom row of Fig. 5). At 06:54 UT the BP is at its peak intensity and the dis-

tance between the two main polarities of the MBF is  $\sim 11''$ .

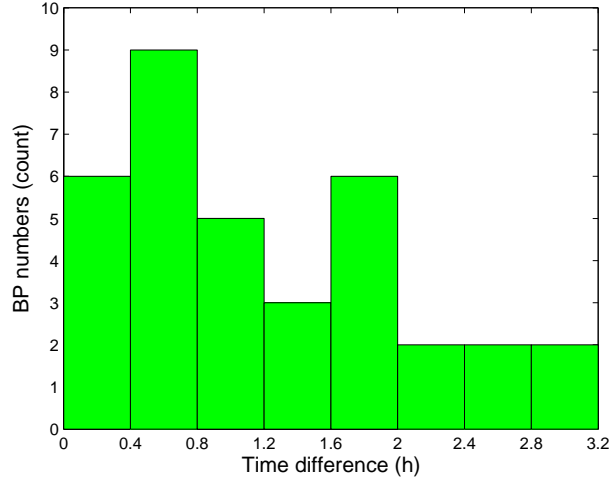


Fig. 6.— Statistical histogram of the time difference between the emergence of MBFs and the appearance of BPs in the cases when the MBF is formed by one bipolar emergence.

### 3.2.2. Time difference between emergence of MBFs and appearance of BPs

From 70 BPs, 35 are associated with MBFs formed by bipolar emergence process. Here, we measured the time difference between the flux emergence and the BP appearance in these 35 cases. A MBF is considered as emerging when it appears and has a flux density above  $30 \text{ Mx cm}^{-2}$ . A statistical histogram of the time difference is shown in Fig. 6. We found that the time difference varies from 0.1 to 3.2 hours with an average of 1.3 hours. The reasons for this time difference might be twofold. First, it takes a certain amount of time for heating the BP plasma to a temperature level at which the AIA 193 Å channel is sensitive. Second, it is possible that it takes some time after the flux emergence that the physical process heating the plasma (thus producing a BP) starts to operate. Since the time scale of plasma heating is normally very small, the second reason is the most plausible, though the first one might work in some cases.

### 3.2.3. A MBF formed by convergence

In Fig. 7, we give an example of a MBF formed by convergence. The MBF is associated with a BP seen in AIA 193 Å from 15:39 UT on January 2 to 07:20 UT on January 3, with a lifetime of about 16 hours. The BP is listed as the No. 42 event in Table 1. Initially, the two polarities are found to be at a distance of about  $23''$  (see image at 07:49 UT in Fig. 7). Then they move

towards each other. When the BP starts to be seen in AIA 193 Å around 16:44 UT, the distance between the two polarities is about  $6''$ . The distance is found to be about  $4''$  when the BP reaches its emission peak in the AIA 193 Å channel (see images at 19:44 UT in Fig. 7). The  $6''$  distance between the two polarities when the BP appears is consistent with what was found by Madjarska et al. (2003).

### 3.2.4. A MBF formed by local coalescence

Fig. 8 shows the evolution of a BP (No. 19 in Table 1) and its associated MBF formed by local coalescence. In this case a few small magnetic flux kernels are first seen (see features denoted by arrows at 05:09 UT in Fig. 8) surrounded by mostly fuzzy, weak magnetic flux concentrations. The kernels coalesce with these magnetic features of the same sign to form larger ones. This process leads to the formation of a BP in AIA 193 Å. The distance between the two polarities remains almost the same, changing slowly during the merging process. The distances measured at 05:09 UT, 10:34 UT and 17:49 UT are  $15''$ ,  $15''$  and  $13''$ , respectively. In the convergence cases, for instance, the distance changes dynamically. These weak magnetic features can not directly trigger a BP until they merge into large ones. These cases are, therefore, different from the emergence cases where the flux emergence is directly followed by a BP formation in the AIA 193 Å.

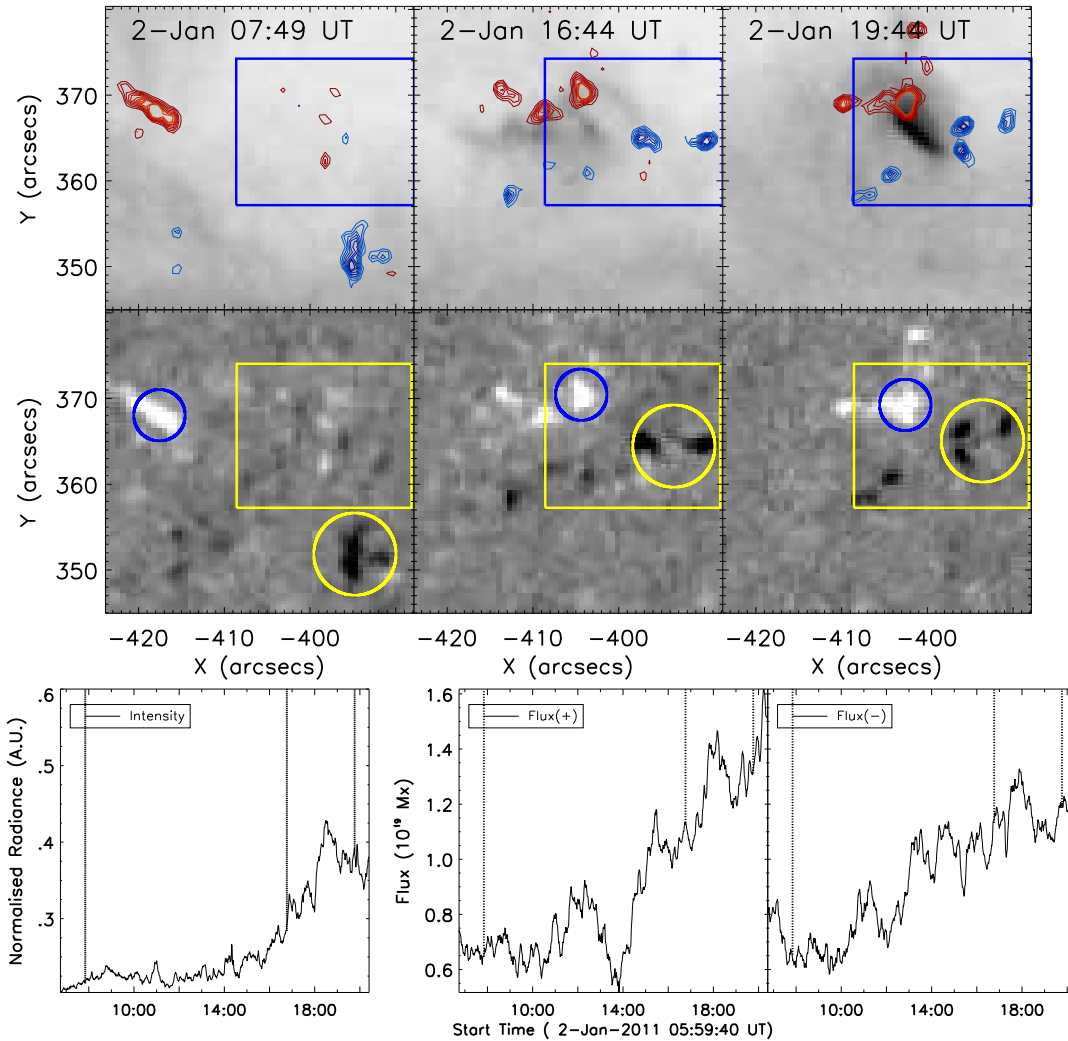


Fig. 7.— Same as Fig. 5, but for the event numbered 42 in Table 1 whose associated MBF is formed through convergence. An animation is enclosed online.

### 3.2.5. Distance of two main polarities of a MBF

As already shown in the above sections, the distance of the two main polarities of the MBFs varies in different stages of the evolution of a BP, and it seems to be dependent on the formation mechanism of the MBFs. In Fig. 9, we show the distances at the time when the BPs are first seen and at their radiation peak in the AIA 193 Å channel. For MBFs formed by convergence, the distances at the radiation peaks are shorter than that at the time of the first appearances. For MBFs formed by local coalescence, the distances at the radiation peaks are also shorter than (or equal to)

those at the first appearance, but the changes are small compared to the convergence cases. The distance variations are more complex for those formed by bipolar emergence. For the 35 bipolar emergence cases, the distances at the time of the first appearance of 25 cases are shorter than, of 4 cases equal to, and of 6 cases longer than those at the radiation peaks. The variation of the distances during a BP lifetime is complex and it might randomly increase/decrease.

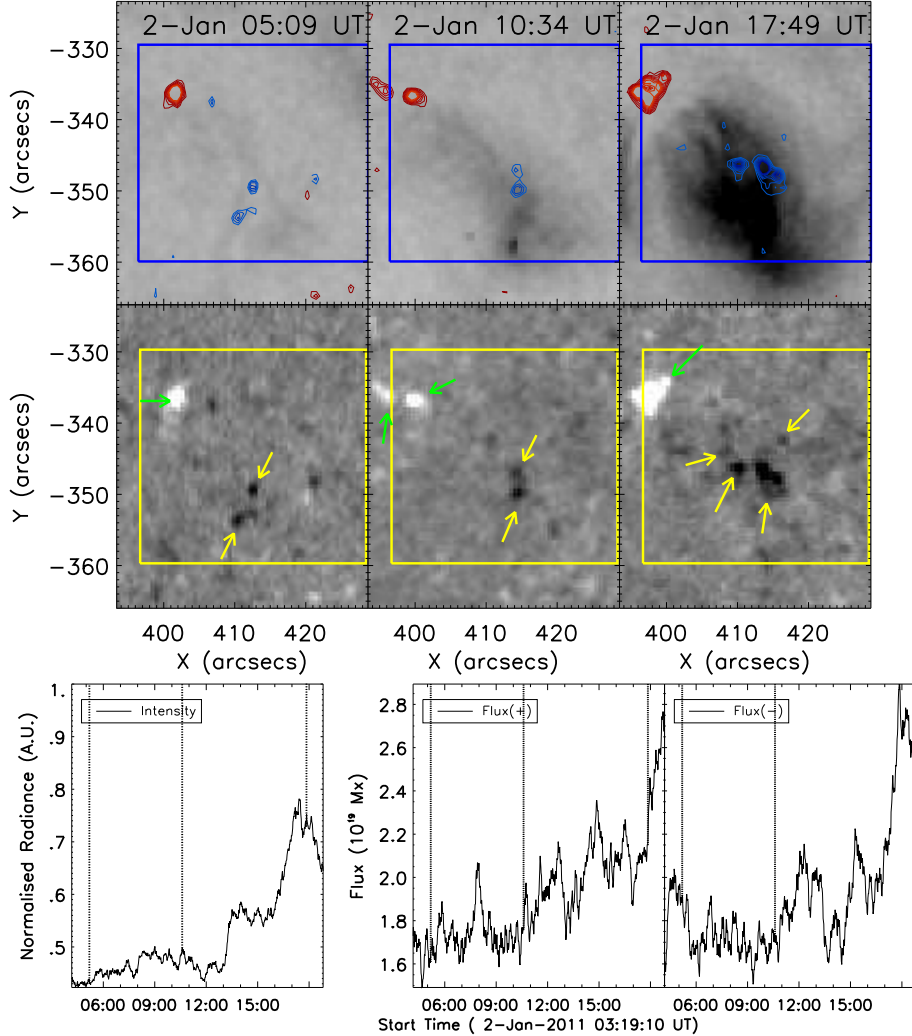


Fig. 8.— Same as Fig. 5, but for the event numbered 19 in Table 1 whose associated MBF is formed through local coalescence. An animation is given online.

### 3.3. Magnetic cancellation associated with BPs

Magnetic cancellation is another phenomenon observed during a BP evolution (see Section 1 for reviews of previous works) and it has been observed in all BPs studied here. Magnetic cancellation is a phenomenological description of a magnetic process that interprets the disappearance and/or decrease of opposite sign magnetic features when they are in contact with each other observed in magnetograms. As pointed out by Harvey et al. (1999), magnetic flux that is retracting below the solar surface in cancellation sites is believed to be an outcome of magnetic reconnection

(Priest & Forbes 2007). Since magnetic cancellation is related to BPs, this suggests that a BP and its associated magnetic cancellation are likely to be the result of magnetic reconnection. Thus, a study on how magnetic cancellation occurs can help to understand how magnetic reconnection process operates to energise a BP.

In our study, we found that it is difficult to identify magnetic cancellation only by following the temporal variation of the magnetic flux in the lightcurves of the total positive and negative fluxes associated with a BP due to the complex magnetic flux evolution in the pho-

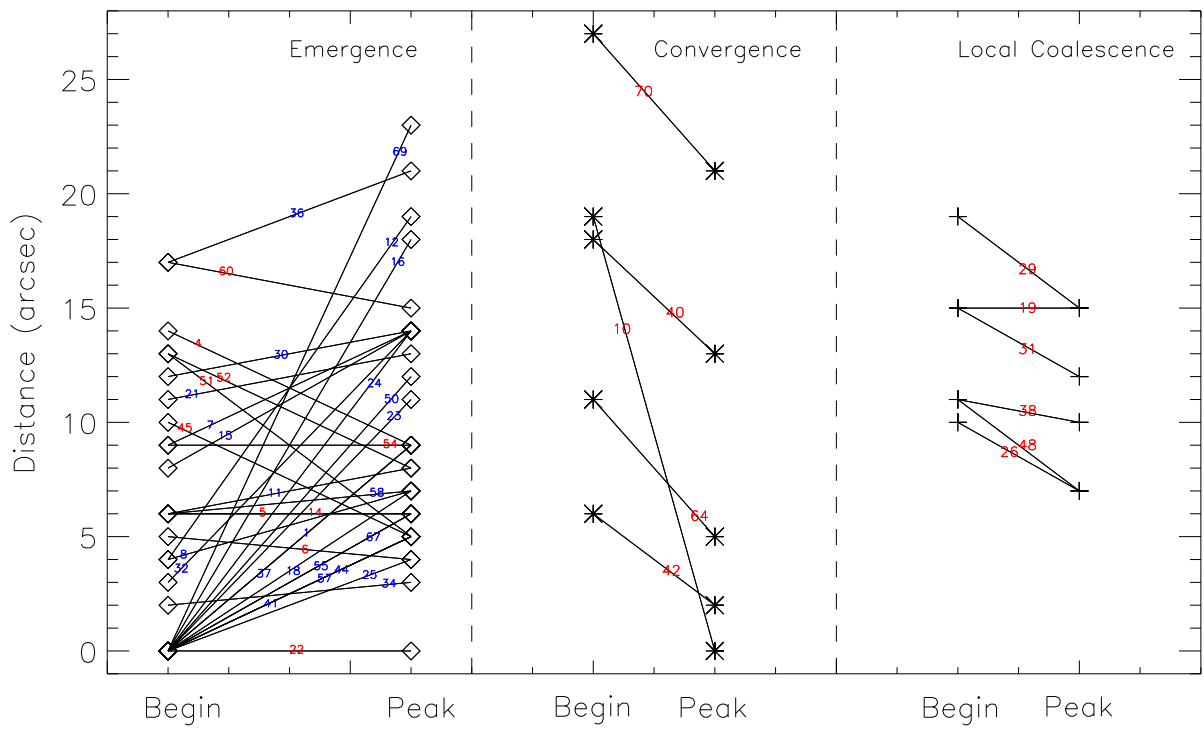


Fig. 9.— Distances of the two main polarities of MBFs formed by emergence (left), convergence (middle) and local coalescence at the time when the BPs are first seen (“begin”) and at their radiation peaks (“peak”) in the AIA 193 Å passband. The denoted numbers are the numbers of the BPs listed in Table 1. The solid line connects the two distances determined at the “begin” and “peak” of an event.

tosphere. Because of the non-potentiality of the magnetic field and the lack of data that are suitable for a non-linear magnetic field extrapolation, potential field extrapolation models will not reproduce the real field configuration of BPs. Thus, the only reliable analysis at present remains a visual inspection of longitudinal magnetograms.

From the analysis of the 70 samples, we found that magnetic cancellation associated with a BP can occur in three different ways: (I) between a MBF and small weak magnetic features that are evolving in the vicinity; (II) within a MBF when the two main polarities are moving towards each other from a large distance; (III) within a MBF whose two main polarities emerge in the same place simultaneously.

Magnetic cancellation of category I and II are found for the majority of our samples. We found that 67 out of 70 cases occur in these two ways of evolutionary pattern. We also noticed that most of the BPs do not follow only a single way. Cancellation associated with categories I and II were found at different time during the evolution of BPs. However, for any individual BP, we could always find one dominant pattern in the cancellation, which is found to occur during most of the BP lifetime. This dominant evolutionary pattern is listed in Table 1. In total, we found that 33 BPs are primarily associated with magnetic cancellation of category I and 34 BPs of category II. Fig. 10 presents a pie-chart of the statistical results of three categories of cancellation.

We also further investigated whether magnetic cancellation occurring in the three different ways of evolutionary patterns affects the BP lifetimes. Because there are very few cases that are related to category III, we only considered the first two categories. In category I, the lifetimes vary from 6.4 hours to 45 hours with an average of 23 hours, and from 2.7 hours to 58.8 hours with an average of 19.6 hours in category II. Although the average lifetime of the BP in category I is a few hours longer, there is no clear correlation between the BP lifetimes and the magnetic cancellation categories. In our investigation, a BP will disappear once one of the main polarities becomes too weak or disappears.

### 3.3.1. A case of category (I)

Fig. 11 shows the evolution of a BP and its associated magnetic features, which present magnetic cancellation occurring between the main MBF and small magnetic features. This BP is the same as the one

presented in Fig. 5 and the attached animation there. In this event, small-scale weak magnetic features are found to play a key role in the BP evolution. In Fig. 11, we show a few snapshots of the BP and its associated magnetic features. These small magnetic features move towards and interact with the main polarities. This process is followed by the disappearance of the small features and is accompanied by emission enhancements in AIA 193 Å. This example suggests that the main MBF builds up the skeleton of the BP but the activity of the small-scale magnetic fluxes is responsible for the BP heating.

Based on the observations shown in Fig. 11, we suggest a cartoon model showing a reconnection process that can explain the observed magnetic cancellation and the BP formation (see Fig. 12). In this model, the large loops are rooted in the main MBF while the small loops connect the small magnetic features (Fig. 12a). The two loop systems move towards each other due to the solar convection. They interact and reconnect with each other (Fig. 12b), which then releases energy to heat the loop system that represents a BP. The reconnection results in a tiny loop that will submerge following the reconnection (Fig. 12c). In this model, the reconnection may occur in the lower solar atmosphere since a small loop is involved. Evidences of magnetic reconnection between two loop systems in the solar atmosphere have been reported by numerous studies, e.g. Huang et al. (2014) and Huang et al. (2015).

### 3.3.2. A case of category (II)

Fig. 13 shows an example where a BP is flared up during the converging motions of the two main polarities. This BP is the same as the one shown in Fig. 7 and its full evolution is given in the attached animation. The event clearly demonstrates that the emission in AIA 193 Å increases when the two main polarities move closer and while are in contact (see image at 00:29 UT in Fig. 13). The magnetic cancellation is found to occur between the two main polarities. When the fluxes of the main polarities are canceled out, the BP disappears. A similar relation between magnetic flux cancellation and BP evolution has been reported in several studies (e.g. Brown et al. 2001; Madjarska et al. 2003; Huang et al. 2012, etc.).

Although two cancelling polarities might connect each other in the initial stage as pointed out in Section 3.2, we assume here that they do not, and then this case can be explained by a BP scenario proposed by

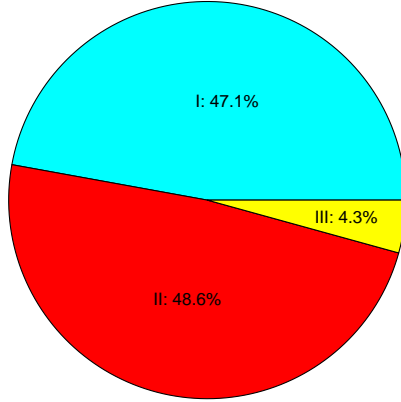


Fig. 10.— A pie-chart to show the three different ways of evolutionary pattern that magnetic cancellation occurs along with 70 studied BPs.

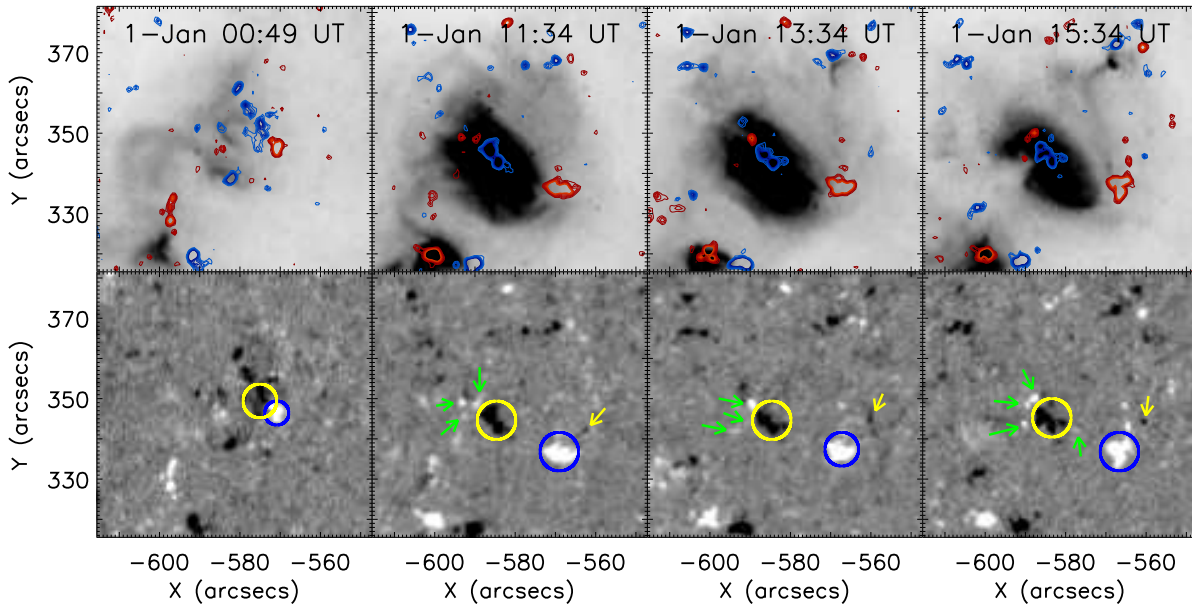


Fig. 11.— An example (No. 1 listed in Table 1) of a BP that is associated with magnetic cancellation occurring between the main polarities of the MBF and small weak features. The BP seen in AIA 193 Å is given in the top row, and its associated magnetograms are given in the bottom row. The contours of positive (red) and negative (blue) magnetic flux density are over-plotted in the top row. The blue and yellow circles mark the main MBF. The yellow and green arrows indicate that the small magnetic features are about to cancel with the polarities of the MBF. This is the same event as shown in Fig. 5 and an animation of this BP is attached to Fig. 5.

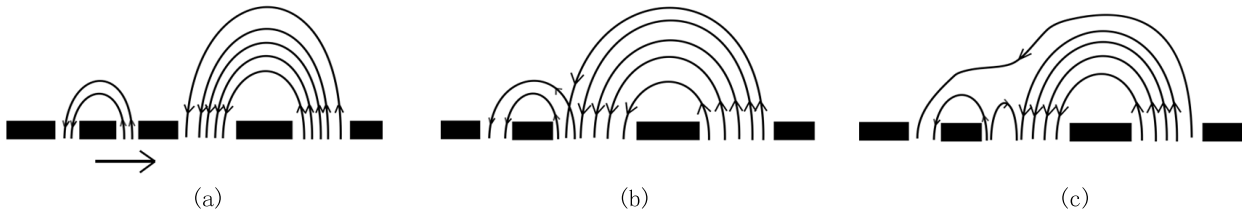


Fig. 12.— A cartoon demonstrating the topological evolution of the magnetic fields which are involved in the magnetic cancellation and BP heating in the case shown in Fig. 11. Panel (a) presents an initial magnetic topology with a large magnetic loop (corresponding to the MBF) and a small one (corresponding to small and weak magnetic features). Panel (b) shows that the large magnetic loops are interacting with the small ones and magnetic reconnection occurs. Panel (c) presents the magnetic field topology after reconnection. The produced small loop will submerge due to the magnetic tension.

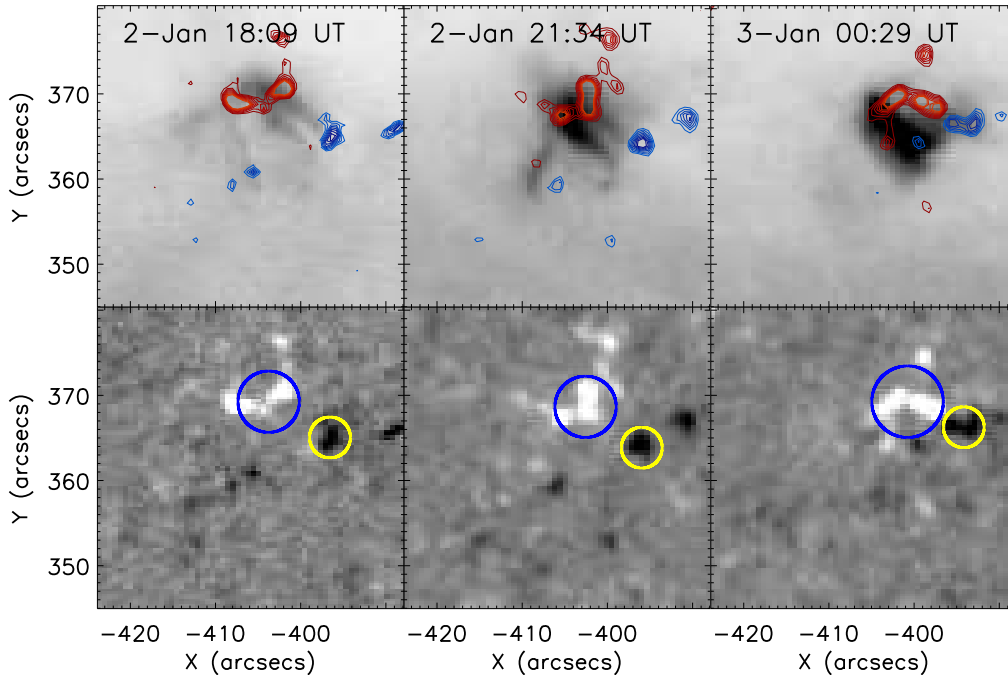


Fig. 13.— Same as Fig. 11, but gives an example of magnetic cancellation occurring between two main polarities of the MBF when they are moving towards each other from a far distance. Its associated BP is numbered as 42 in Table 1. This is the same event as shown in Fig. 7, and an animation is given online attached to Fig. 7.

Priest et al. (1994). We give a simplified version of their model in Fig. 14. The initial configuration of the model consists of two magnetic loop systems. Each of them has one footpoint rooted in one of the polarities of the main MBF (Fig. 14a). The converging motion forces the loops to move closer and their field

lines to reconnect (Fig. 14b). The resulting small magnetic loops connecting the two main polarities of MBF then submerge. The fluxes in the main polarities are canceled out by this process (Fig. 14c). In this scenario, a BP is produced in the reconnection site and the resulting long loop is not entirely heated by the

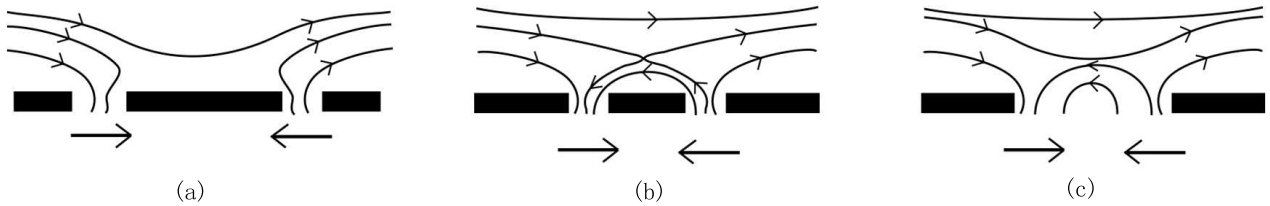


Fig. 14.— A cartoon presenting the evolution of the magnetic field that can explain the magnetic cancellations and the BP shown in Fig. 13. Panel (a) shows that two polarities in the MBF belong to two different loop systems. The convergence motion forces them to move closer, which leads to magnetic reconnection shown in panel (b). The magnetic reconnection heats the BP and the generating small loop will submerge (panel c).

reconnection process. For more details on the convergence model (Fig. 14) please refer to [Priest et al. \(1994\)](#) and their follow-up works ([Parnell et al. 1994](#); [von Rekowski et al. 2006a,b](#)).

### 3.3.3. A case of category (III)

Magnetic cancellation occurring in category III is relatively rare (only 3 out of 70 cases). In this category, the magnetic cancellation happens between the two main polarities of a MBF. However, it differs from the category II because here the two main polarities emerge in the same location simultaneously (i.e. bipolar emergence). This indicates that magnetic loops have been connecting them since their birth. In this case, the emerged main polarities first move away from each other and a BP appears in the images of the AIA 193 Å channel. Further in the evolution of the BP the two main polarities move towards each other which initiates magnetic cancellation.

Fig. 15 displays a BP (No. 22 in Table 1) which belongs to category III. The BP starts to be seen in AIA 193 Å at 02:18 UT on January 1 while its MBF is emerging. The two polarities of the MBF are at zero distance, i.e. the two polarities touch each other. While the two main polarities move away from each other, the BP increases in both size and emission. At 03:20 UT, the two main polarities have a maximum separation of about  $10''$ . After, they start to move towards each other, and magnetic cancellation occurs between them, while the BP becomes brighter. We also observed a shearing motion that occurs while the two polarities move closer (see Fig. 15). The BP reaches its emission peak at around 03:50 UT when the two main polarities are again in contact. The BP lasts until 10:18 UT when the flux in the positive polarity is nearly canceled out.

To determine whether the magnetic cancellation observed in this case is associated with magnetic reconnection that energises the BP can be challenging. In Fig. 16, we present a cartoon layout of magnetic fields involved in magnetic reconnection that can generate energy to heat the BP. In this cartoon, the magnetic loops are initially connecting the two main polarities (Fig. 16a). Converging motions then force the field lines to reconnect (Fig. 16b) due to instabilities (for example, kink instability due to shearing motion). The reconnection will result in a smaller loop that will submerge and a magnetic island that will be ejected from the reconnection site (Fig. 16c). This model can be considered as a micro version of a flare model proposed by [Hirayama \(1974\)](#). The ejected magnetic island is the main phenomenon that can be used to test the scenario. It can generate a so-called blowout jet (see example given in [Young & Muglach 2014](#)) or a mini-CME (see example given in [Innes et al. 2010](#)). We then searched for observational signatures of such a phenomenon by tracing the evolution of the BP in AIA 193 Å. Ejections of plasma similar to blowout jet are present from time to time throughout the BP lifetime duration (see online animation attached to Fig. 15). An example is given in the image at 03:53 UT of Fig. 15, where the front of a fuzzy arch-like feature is outlined. The structure is moving away from the BP, and that can be followed in the attached online animation. Observational evidence for instabilities are needed to fully prove this scenario, but this is beyond the scope of the current study.

## 4. Conclusion and Summary

In the present study, we aim to investigate how a BP-associated MBF is formed and how magnetic cancellation associated with BPs occurs. We have traced

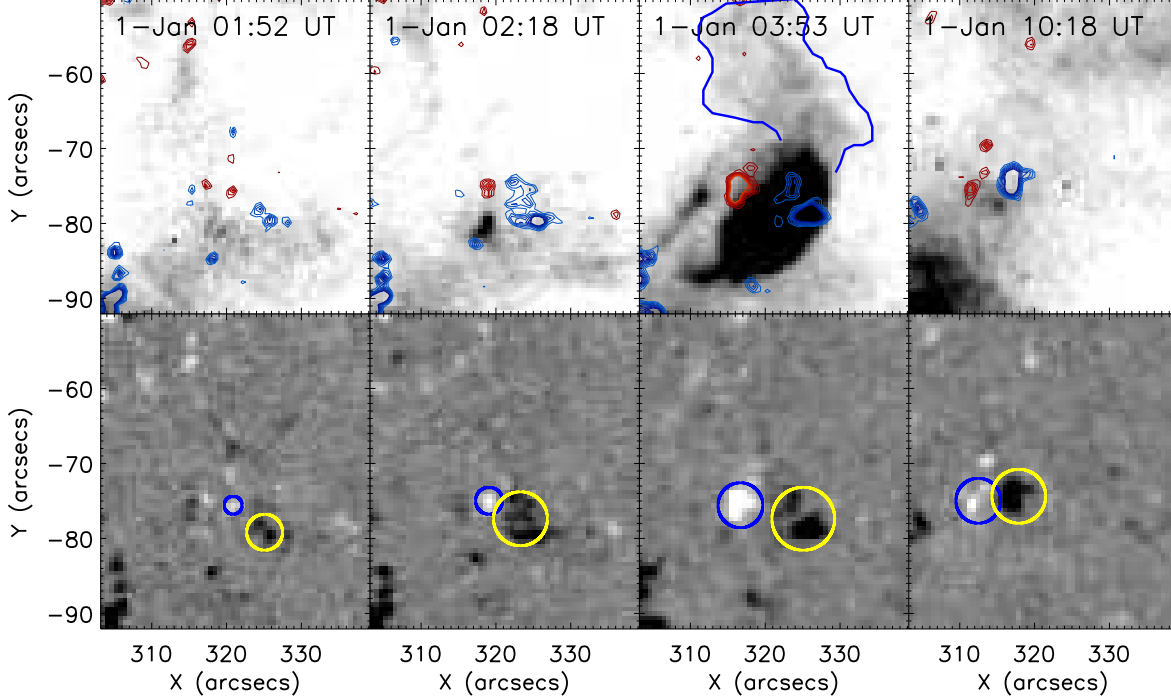


Fig. 15.— An example showing the evolution of a BP (No. 22 listed in Table 1) and its associated magnetic features. This is an example whose associated magnetic cancellation occurs within two main polarities of the MBF that emerged from the same location simultaneously. The BP images seen in AIA 193 Å are given in the top row and the magnetograms are given in the bottom row. The blue and yellow circles mark the polarities of the MBF. The contours of positive (red) and negative (blue) magnetic flux density are over-plotted in the top row. The blue line in the AIA image at 03:53 UT denotes a blowout plasma structure originated from the BP. An animation is given online.

the evolution of 70 BPs throughout their lifetimes together with their associated photospheric magnetic flux using SDO/AIA and SDO/HMI observations.

We found that the lifetimes of the BPs vary from 2.7 to 58.8 hours averaging at 20.9 hours. The distance of the two opposite polarities of a MBF associated with these BPs changes throughout the BP lifetime. When the BPs first appear, the distance distributes in the range from 0 to 31.5". A zero distance is found in 16 BP-associated MBFs from which 15 are related to bipolar flux emergence. The distance spreads from 0" to 26.8" with a peak of the distribution at 5" when the BPs are at their radiation peak.

We found that a BP-associated MBF can be formed in three ways: emergence where a magnetic feature appears and grows as seen in the HMI magnetograms,

convergence where the two pre-existing polarities move towards each other from a large distance, and local coalescence where a magnetic feature is formed by merge with several small magnetic flux concentrations of the same sign.

Out of the 70 cases, flux emergence is the main process of a MBF buildup for 52 BPs, mainly convergence is seen in 28 BPs, and 14 cases are associated with local coalescence. For those BPs whose two polarities are purely formed by the same mechanism (46 cases), 35 cases are related to bipolar emergence, 5 cases are formed by convergence and 6 cases by local coalescence. In the 35 cases, the time difference between first appearance of the BPs in AIA 193 Å and the flux emergence ranges from 0.1 to 3.2 hours with an average of 1.3 hours.

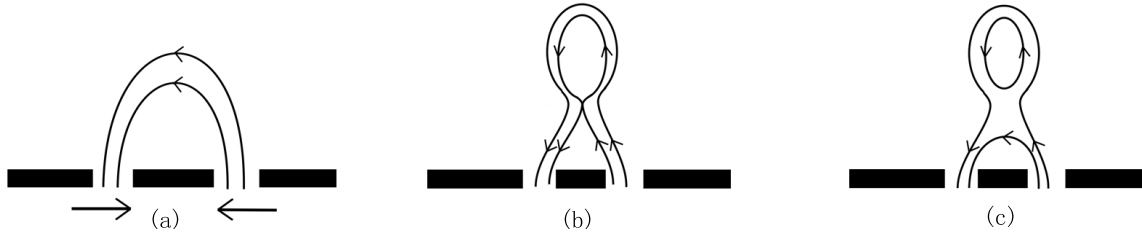


Fig. 16.— A cartoon showing a magnetic reconnection process that may be responsible for the magnetic cancellation and the plasma ejection presented in Fig. 15. Panels (a), (b) and (c) display the initial stage, the reconnection and the resultant magnetic field.

We further investigated the distance between the two main polarities of a MBF at the time when the BPs were first visible and when they were at their radiation peak in the AIA 193 Å channel. In the cases of convergence we found that the distance at the time when the BP is first visible is much longer than that at the radiation peak. In the cases of local coalescence, the distances are more or less the same. In a total of 35 cases of bipolar emergence, the distances at the first appearance of 25 are shorter than, 4 are equal to, and 6 are longer than that at the BP's radiation peaks. The variation of the distances during a BP lifetime might randomly increase/decrease.

All 70 BPs are found to be associated with magnetic cancellation. However, magnetic cancellation associated with BPs can occur in three ways: (I) between the main polarities of a MBF and small weak magnetic fields, (II) between the two polarities of a main MBF while they are moving towards each other from a large distance, and (III) between two polarities of a MBF that emerge together at the same location. Out of 70 BPs, in 33 cases magnetic cancellation primarily occurs in category I, in 34 cases in category II, and 3 cases belong to category III. For each category, we displayed a cartoon model that can explain the observed magnetic cancellation and reconnection responsible for the heating of the BPs. While the main polarities of a BP-associated MBF build up the skeleton of a BP, we find that the magnetic activities responsible for the BP heating may involve small weak fields.

*Acknowledgments:* We thank very much the anonymous referee for his/her helpful and constructive comments. We also thank Dr. Armin Theissen for his linguistic corrections. We thank Dr. Kamalam Vanninathan and Dr. Kalugodu Chandrashekhara for carefully reading the manuscript, and their useful com-

ments and suggestions. This research is supported by the China 973 program 2012CB825601, the National Natural Science Foundation of China under contracts: 41404135 (ZH), 41274178 and 41474150 (LX & ZH), and 41174154, 41274176 and 41474149 (BL), the Shandong provincial Natural Science Foundation ZR2014DQ006, China Postdoctoral Science Foundation funded project and special funds from Shandong provincial postdoc innovation project (ZH). MM is supported by the Leverhulme Trust. Research at the Armagh Observatory is grant-aided by the N. Ireland Department of Culture, Arts and Leisure. AIA and HMI data is courtesy of SDO (NASA). We thank JSOC for providing downlinks of the SDO data.

*Facilities:* SDO.

## REFERENCES

- Alexander, C. E., Del Zanna, G., & Maclean, R. C. 2011, *A&A*, 526, A134
- Brown, D. S., Parnell, C. E., Deluca, E. E., Golub, L., & McMullen, R. A. 2001, *Sol. Phys.*, 201, 305
- Chandrashekhara, K., Krishna Prasad, S., Banerjee, D., Ravindra, B., & Seaton, D. B. 2013, *Sol. Phys.*, 286, 125
- DeForest, C. E., Hagenaar, H. J., Lamb, D. A., Parnell, C. E., & Welsch, B. T. 2007, *ApJ*, 666, 576
- Golub, L., Krieger, A., Simon, R., Vaiana, G., & Timothy, A. F. 1975a, in *Bulletin of the American Astronomical Society*, Vol. 7, *Bulletin of the American Astronomical Society*, 350
- Golub, L., Krieger, A. S., Harvey, J. W., & Vaiana, G. S. 1977, *Sol. Phys.*, 53, 111

- Golub, L., Krieger, A. S., & Vaiana, G. S. 1976a, in IAU Symposium, Vol. 71, Basic Mechanisms of Solar Activity, ed. V. Bumba & J. Kleczek, 145
- Golub, L., Krieger, A. S., & Vaiana, G. S. 1976b, Sol. Phys., 49, 79
- Golub, L., Krieger, A. S., Silk, J. K., Timothy, A. F., & Vaiana, G. S. 1975b, in IAU Symposium, Vol. 68, Solar Gamma-, X-, and EUV Radiation, ed. S. R. Kane, 23
- Habbal, S. R., Dowdy, Jr., J. F., & Withbroe, G. L. 1988, in Bulletin of the American Astronomical Society, Vol. 20, Bulletin of the American Astronomical Society, 977
- Habbal, S. R., & Withbroe, G. L. 1981, Sol. Phys., 69, 77
- Habbal, S. R., Withbroe, G. L., & Dowdy, Jr., J. F. 1990, ApJ, 352, 333
- Harvey, K. L., Jones, H. P., Schrijver, C. J., & Penn, M. J. 1999, Sol. Phys., 190, 35
- Hirayama, T. 1974, Sol. Phys., 34, 323
- Huang, Z., Madjarska, M. S., Doyle, J. G., & Lamb, D. A. 2012, A&A, 548, A62
- Huang, Z., Madjarska, M. S., Xia, L., et al. 2014, ApJ, 797, 88
- Huang, Z., Xia, L., Li, B., & Madjarska, M. S. 2015, ApJ, 810, 46
- Innes, D. E., McIntosh, S. W., & Pietarila, A. 2010, A&A, 517, L7
- Krieger, A. S., Vaiana, G. S., & van Speybroeck, L. P. 1971, in IAU Symposium, Vol. 43, Solar Magnetic Fields, ed. R. Howard, 397
- Lamb, D. A., DeForest, C. E., Hagenaar, H. J., Parnell, C. E., & Welsch, B. T. 2008, ApJ, 674, 520
- . 2010, ApJ, 720, 1405
- Lamb, D. A., Howard, T. A., DeForest, C. E., Parnell, C. E., & Welsch, B. T. 2013, ApJ, 774, 127
- Lemen, J. R., Title, A. M., Akin, D. J., et al. 2012, Sol. Phys., 275, 17
- Liu, Y., Hoeksema, J. T., Scherrer, P. H., et al. 2012, Sol. Phys., 279, 295
- Madjarska, M. S., Doyle, J. G., Teriaca, L., & Banerjee, D. 2003, A&A, 398, 775
- Madjarska, M. S., Huang, Z., Doyle, J. G., & Subramanian, S. 2012, A&A, 545, A67
- Martin, S. F., & Harvey, K. H. 1979, Sol. Phys., 64, 93
- McIntosh, S. W. 2007, ApJ, 670, 1401
- Parnell, C. E., Priest, E. R., & Titov, V. S. 1994, Sol. Phys., 153, 217
- Pérez-Suárez, D., Maclean, R. C., Doyle, J. G., & Madjarska, M. S. 2008, A&A, 492, 575
- Pesnell, W., Thompson, B., & Chamberlin, P. 2012, Sol. Phys., 275, 3
- Pevtsov, A. A., Fisher, G. H., Acton, L. W., et al. 2003, ApJ, 598, 1387
- Preś, P., & Phillips, K. H. J. 1999, ApJ, 510, L73
- Priest, E., & Forbes, T. 2007, Magnetic Reconnection (UK: Cambridge University Press)
- Priest, E. R., Parnell, C. E., & Martin, S. F. 1994, ApJ, 427, 459
- Scherrer, P. H., Schou, J., Bush, R. I., et al. 2012, Sol. Phys., 275, 207
- Sheeley, Jr., N. R., & Golub, L. 1979, Sol. Phys., 63, 119
- Timothy, A., Golub, L., Krieger, A., Silk, J. K., & Vaiana, G. 1974, in Bulletin of the American Astronomical Society, Vol. 6, Bulletin of the American Astronomical Society, 265
- Ugarte-Urra, I., & Doyle, J. G. 2004, in ESA Special Publication, Vol. 575, SOHO 15 Coronal Heating, ed. R. W. Walsh, J. Ireland, D. Danesy, & B. Fleck, 535
- Vaiana, G. S., Krieger, A. S., Van Speybroeck, L. P., & Zehnpfennig, T. 1970, Bull. Am. Phys. Soc., 15, 611
- von Rekowski, B., Parnell, C. E., & Priest, E. R. 2006a, MNRAS, 366, 125
- . 2006b, MNRAS, 369, 43
- Webb, D. F., Martin, S. F., Moses, D., & Harvey, J. W. 1993, Sol. Phys., 144, 15

Young, P. R., & Muglach, K. 2014, *Sol. Phys.*, 289, 3313

Zhang, J., Kundu, M. R., & White, S. M. 2001, *Sol. Phys.*, 198, 347

Zhang, Q. M., Chen, P. F., Ding, M. D., & Ji, H. S. 2014, *A&A*, 568, A30

Zhang, Q. M., Chen, P. F., Guo, Y., Fang, C., & Ding, M. D. 2012, *ApJ*, 746, 19

Table 1:: The studied BPs, formations of their associated MBFs, and magnetic cancellations associated with heating.

No.	Location (x,y) [arcsec]	Start Time	End time	Duration (hours)	Bipolar formation*		Cancel- lation*	Distance of main polarities (arcsec)	
					Positive	Negative		Beginning*	Peak*
1	-542, 338	01-01 00:04	01-02 13:19	37.3	A	A	I	0	9
2	-289, 490	01-01 22:26	01-03 23:58	49.5	C+B	B	II	32	27
3	310, -119	01-01 10:29	01-03 21:19	58.8	B	A+B	II	12	9
4	130, -169	01-02 18:09	01-03 09:00	14.9	A	A	I	14	9
5	60, -134	01-01 07:03	01-02 00:10	17.1	A	A	I	6	6
6	-34, -204	01-01 11:53	01-02 23:50	36.0	A	A	I	5	4
7	170, -229	01-01 14:43	01-02 18:50	28.1	A	A	I	9	14
8	-109, -209	01-01 20:00	01-02 16:40	20.7	A	A	I	4	7
9	140, -109	01-02 21:39	01-03 23:59	26.3	A+B	B	I	6	8
10	-89, -69	01-01 14:58	01-02 07:10	16.2	B	B	II	19	0
11	95, -164	01-01 11:24	01-02 12:30	25.1	A	A	I	6	8
12	205, -94	01-02 04:04	01-03 05:40	25.6	A	A	I	4	19
13	-59, -449	12-31 23:48	01-01 17:30	17.7	B	A+B	II	8	8
14	340, -389	01-01 16:25	01-02 11:30	19.1	A	A	III	6	6
15	180, -224	01-01 14:58	01-02 20:10	29.2	A	A	I	8	14
16	155, -329	01-01 20:15	01-03 08:10	35.9	A	A	I	0	18
17	255, -369	01-02 11:54	01-03 01:20	13.4	B	A+B	II	8	3
18	275, -319	01-02 06:44	01-03 09:10	26.4	A	A	I	0	7
19	480, -339	01-02 12:54	01-03 09:00	20.1	C	C	II	15	15
20	270, -359	01-02 10:14	01-03 03:50	17.6	B	A+B	II	13	19
21	290, -99	12-31 22:10	01-01 23:30	25.3	A	A	I	11	13
22	340, -79	01-01 02:12	01-01 10:19	8.1	A	A	III	0	0
23	660, -169	01-02 11:19	01-03 06:40	19.4	A	A	I	0	11
24	630, -179	01-02 17:09	01-03 07:30	14.4	A	A	I	0	14
25	770, 45	01-02 17:59	01-03 12:00	18.0	A	A	I	0	4
26	160, -144	01-01 03:08	01-02 00:50	21.7	C	C	II	10	7
27	440, -164	01-01 11:18	01-02 00:20	13.0	C+B	B	II	9	4
28	740, 0	01-02 15:28	01-03 04:00	12.5	C+B	B	II	13	5
29	520, 30	01-01 23:10	01-02 19:50	20.7	C	C	II	19	15
30	510, -49	01-02 19:34	01-03 17:00	21.4	A	A	I	12	14
31	510, -129	01-02 21:35	01-03 09:20	11.8	C	C	II	15	12
32	645, -64	01-03 00:59	01-03 15:30	14.5	A	A	I	3	14
33	100, -169	12-31 21:58	01-01 20:40	22.7	B	A+B	II	16	7
34	-359, 510	01-01 07:48	01-01 14:29	6.7	A	A	III	2	3
35	-264, 345	01-01 16:00	01-03 01:40	33.7	A+B	B	II	20	9
36	-234, 380	01-02 00:25	01-03 06:20	29.9	A	A	I	17	21
37	-199, 380	01-01 17:35	01-02 11:20	17.8	A	A	I	0	9
38	-509, 475	01-01 08:48	01-01 21:50	13.0	C	C	II	11	10
39	-339, 400	01-01 00:43	01-03 03:30	50.8	B	A+B	II	0	12
40	-124, 405	01-03 08:24	01-03 23:59	15.6	B	B	II	18	13
41	-359, 335	01-02 10:49	01-03 17:00	30.2	A	A	I	0	5
42	-319, 370	01-02 15:39	01-03 07:20	15.7	B	B	II	6	2
43	-629, 340	01-01 03:33	01-01 17:10	13.6	B	C+B	II	14	9
44	-469, 540	01-02 00:30	01-02 19:40	19.2	A	A	I	0	5
45	-549, 320	12-31 17:58	01-01 23:20	29.4	A	A	I	10	5
46	-149, 430	01-02 16:09	01-03 02:00	9.9	A+B	B	II	11	4
47	0, 580	01-03 03:59	01-03 12:50	8.9	C+B	B	II	18	11
48	-454, 145	01-01 09:48	01-01 18:50	9.0	C	C	II	11	7
49	-484, 125	01-01 08:38	01-02 01:50	17.2	A+B	B	II	4	9
50	-379, 205	12-31 20:29	01-01 20:20	23.9	A	A	I	0	12
51	-344, 295	01-01 00:38	01-01 17:40	17.0	A	A	I	13	5
52	-449, 235	12-31 13:59	01-02 17:30	51.5	A	A	I	13	8
53	-429, 205	01-01 14:43	01-02 01:40	11.0	A+B	B	II	16	0
54	-349, 180	01-01 23:04	01-02 14:50	15.8	A	A	I	9	9
55	-289, 90	01-02 07:35	01-02 14:00	6.4	A	A	I	0	6
56	-194, 210	01-02 13:39	01-02 17:40	4.0	A+B	B	II	6	5
57	-239, 310	01-02 12:04	01-03 14:50	26.8	A	A	I	0	5
58	-174, 165	01-02 12:18	01-03 01:30	13.2	A	A	I	6	7
59	-14, 305	01-03 02:09	01-03 20:40	18.5	B	A+B	II	16	12
60	-79, 260	01-02 18:08	01-03 18:00	23.9	A	A	I	17	15
61	-254, 315	01-01 22:55	01-02 23:30	24.6	B	A+B	II	16	6
62	-479, 210	01-01 10:18	01-01 12:59	2.7	A+B	B	II	12	5
63	-434, 295	12-31 15:49	01-01 12:09	20.3	C+B	B	II	22	6
64	-469, 240	01-01 06:28	01-01 15:50	9.4	B	B	II	11	5
65	-249, 230	01-01 09:08	01-01 23:20	14.2	B	A+B	II	14	11

Continued on next page

**Table 1 – continued**

No.	Location (x,y) [arcsec]	Start Time	End time	Duration (hours)	Bipolar formation <sup>◆</sup>		Cancel- lation <sup>★</sup>	Distance of main polarities (arcsec)	
					Positive	Negative		Beginning <sup>*</sup>	Peak <sup>*</sup>
66	-49, 800	01-01 06:03	01-02 10:40	28.6	C	A	II	11	3
67	-181, 655	01-01 16:30	01-02 14:10	21.7	A	A	I	0	6
68	45, 705	01-02 04:24	01-03 04:10	23.8	C+B	B	II	28	24
69	20, 690	01-02 18:04	01-03 05:30	11.4	A	A	I	0	23
70	-144, 615	01-01 21:15	01-02 14:20	17.1	B	B	II	27	21

◆ Formation of a MBF. A: emergence; B: convergence; C: local coalescence  
 ★ Magnetic cancellation associated with BP heating occurs:  
   I: between the MBF and small weak fields;  
   II: within the main polarities of a MBF moving from far distance;  
   III: within the main polarities of a MBF emerging in the same location.  
 \* Beginning: when a BP starts to be seen in AIA 193 Å.  
 ★ Peak: when a BP is seen at its emission peak in AIA 193 Å.